Human Molecular Genetics, 2009, Vol. 18, No. 17 **3244–3256**
doi:10.1093/hmg/ddp262
Advance Access published on June 3, 2009

Golgi function and dysfunction in the first COG4-deficient CDG type II patient

Ellen Reynders[1,†], François Foulquier[2,†], Elisa Leão Teles[3], Dulce Quelhas[4], Willy Morelle[2], Cathérine Rabouille[5], Wim Annaert[1,*,†] and Gert Matthijs[6,*,†]

[1]Laboratory for Membrane Trafficking, Center for Human Genetics, University of Leuven and Department for Molecular and Developmental Genetics, VIB, B-3000 Leuven, Belgium, [2]Laboratoire de Glycobiologie Structurale et Functionelle, USTL, Lille, France, [3]Department of Pediatrics, San João Hospital, Porto, Portugal, [4]Institute of Medical Genetics Jacinto de Magalhães, Porto, Portugal, [5]Department of Cell Biology and Institute of Biomembranes, University Medical Center Utrecht, The Cell Microscopy Center, Utrecht, The Netherlands and [6]Laboratory for Molecular Diagnosis, Center for Human Genetics, University of Leuven, B-3000 Leuven, Belgium

Received January 27, 2009; Revised and Accepted June 1, 2009

The conserved oligomeric Golgi (COG) complex is a hetero-octameric complex essential for normal glycosylation and intra-Golgi transport. An increasing number of congenital disorder of glycosylation type II (CDG-II) mutations are found in COG subunits indicating its importance in glycosylation. We report a new CDG-II patient harbouring a p.R729W missense mutation in COG4 combined with a submicroscopical deletion. The resulting downregulation of COG4 expression additionally affects expression or stability of other lobe A subunits. Despite this, full complex formation was maintained albeit to a lower extent as shown by glycerol gradient centrifugation. Moreover, our data indicate that subunits are present in a cytosolic pool and full complex formation assists tethering preceding membrane fusion. By extending this study to four other known COG-deficient patients, we now present the first comparative analysis on defects in transport, glycosylation and Golgi ultrastructure in these patients. The observed structural and biochemical abnormalities correlate with the severity of the mutation, with the COG4 mutant being the mildest. All together our results indicate that intact COG complexes are required to maintain Golgi dynamics and its associated functions. According to the current CDG nomenclature, this newly identified deficiency is designated CDG-IIj.

INTRODUCTION

The Golgi apparatus is an important relay station in the secretory pathway as it plays a pivotal role in targeting proteins and lipids to distinct post-Golgi compartments (1). During transit through the Golgi apparatus, most of the newly synthesized secretory and membrane-bound proteins undergo major modifications, mainly involving different types of glycosylation. One of these, *N*-glycosylation, is a complex series of reactions, starting in the endoplasmic reticulum (ER) with the formation of a $Glc_3Man_9GlcNAc_2$-PP-Dolichol structure, which is subsequently transferred onto newly synthesized proteins (2). Upon exit from the ER and arrival in the Golgi, these unprocessed *N*-glycan chains are trimmed and modified to give rise to distinct types of complex *N*-glycan structures. Most of the other types of glycosylation, like the formation of *O*- and *C*-glycans, are restricted to either the ER or the Golgi apparatus. To maintain the directional flow of transport, essential for these modifications, the Golgi apparatus is built out of stacked cisternae, laterally interlinked via fenestrated continuities. The differential distribution of proteins and enzymes over these stacks provides the Golgi complex with a *cis*-to-*trans*

*To whom correspondence should be addressed at: Center for Human Genetics, KULeuven, Herestraat 49, B-3000 Leuven, Belgium (GM.)/Center for Human Genetics, KULeuven, and Department of Molecular and Developmental Genetics, VIB, Herestraat 49, B-3000 Leuven, Belgium (W.A.). Tel: +32 16346070 (G.M.)/+32 16330520 (W.A.); Fax: +32 16346060 (G.M.)/+32 16330522 (W.A.); Email: gert.matthijs@uz.kuleuven.be (G.M.)/wim.annaert@cme.vib-kuleuven.be (W.A.)
†The authors wish it to be known that, in their opinion, the first two and last two authors should be regarded as joint First/Last Authors.

polarity (3). A tightly regulated organization of transport is required in order to mediate cargo transit as well as to maintain the *cis*-to-*trans* organization. The exact mechanism of this transit is still not clarified, though it will most likely be a combination of the vesicular transport model, which implicates fixed cisternae with vesicles transporting cargo forward and recycling escaped proteins to earlier cisternae or the ER (4–7) and the cisternal maturation model. In the latter model, the cisternae mature towards the *trans*-side while vesicles constantly recycle enzymes back to earlier compartments (8,9). More recently a two-phase membrane system was proposed in which small soluble cargo distributes equally across the stack and membrane proteins prefer certain cisternae only based on, for instance, the local lipid composition and length of the transmembrane domain (10). Irrespective of the different models and its specificity and directionality, intra-Golgi transport requires a large number of proteins and protein complexes. These include COPI-coat proteins and associated small GTPases, like ARF1 mediating budding/fission, as well as 'Soluble NSF attachment protein receptor' family members that govern vesicle fusion. The targeting specificity is often organized through the concerted action of GTP-bound Rab proteins with so-called tethering complexes, which are soluble multimeric complexes, coupling incoming organelles with the fusion site. One example is the exocyst complex that acts as a tethering complex at the cell surface of budding yeast and in mammalian cells. The main tethering complexes in the early secretory pathway are the 'Transport Protein Particle' (TRAPP) I and II complexes which couple ER-derived vesicles to the ER-Golgi intermediate compartment and the conserved oligomeric Golgi (COG) complex which appears to function in intra-Golgi and/or Golgi-to-ER trafficking.

The COG complex is an octameric hetero-oligomer conserved from yeast to mammals and presents as a bi-lobed structure bridged through the COG1–COG8 interaction (11,12). Deficiencies in single subunits lead to impaired functioning of the COG complexes, concomitant defects in Golgi morphology (13) and affecting the correct functioning of the cell or entire organism. For instance, a deficiency of COG1 or COG2 in CHO cell lines showed a defective retrograde Golgi-to-ER transport, a subsequent disturbance of the Golgi morphology and a destabilization of several proteins, including glycosylation enzymes, thus causing glycosylation abnormalities. The importance of COG function in intra-Golgi transport and its secondary implications on glycosylation are furthermore underscored by the discovery of mutations in the genes encoding the COG1, COG7 and COG8 subunits that were linked to congenital disorders of glycosylation (CDG) (12,14–19). CDG is a rare, recessive disorder first described in 1980 (20,21). Since then, 22 subtypes have been described, which can be divided into two different groups: CDG type I and type II. CDG type I (CDG-I) is caused by defects in enzymes governing the synthesis and transfer of the oligosaccharide in the ER. On the other hand, defects leading to CDG-II have been shown to belong to different classes: enzymes responsible for the modifications of the *N*-glycan chain in the Golgi apparatus, sugar transporters in the Golgi membrane and complexes essential for intra-Golgi and retrograde Golgi-to-ER transport such as the COG complex.

Here we describe a patient harbouring a heterozygous point mutation in the *COG4* gene combined with a deletion on the maternal allele. Experiments performed on this patient's fibroblasts yielded similar defects albeit less severe as found in the cells of the previously described COG-deficient patients. Moreover, we present an updated overview of the different *COG* mutations identified thus far in which we attempt to correlate for the first time the respective clinical phenotypes with the severity in glycosylation and trafficking defects as well as with the Golgi integrity using transmission electron microscopy (TEM). Our analysis underscores the high importance of an intact COG complex in both intra-Golgi trafficking and the maintenance of the normal morphology of the Golgi apparatus. Furthermore, we provide novel insights in the steady-state localization of both full and partial complexes with implications on the action mechanism of the complex. With this study, the number of patients harbouring mutations in individual COG genes rises to ten, which is about one-third of the total number of CDG-II cases in which a mutation has been identified making *COG* mutations one of the most frequent causes of CDG-II. Furthermore, given the insights that the different individual studies have generated on COG complex formation and functioning, we are now at a point where a comparison of all mutant subunits along different criteria reveals more specific or even as yet unknown functions of not only the full complex, but also of different subunits and subcomplexes.

RESULTS

Genetic and molecular analysis of COG4

The identification of several CDG type II patients harbouring mutations in individual subunits of the octameric COG complex fostered a strong interest in the functional role this Golgi tethering complex plays in the glycosylation process. By direct sequencing of the *COG* genes in a cohort of unsolved CDG-II patients, we identified a novel patient carrying a seemingly homozygous C>T point mutation at position 2185 in the genomic DNA encoding the *COG4* gene (Fig. 1A). The mutation was not found after sequencing of over 100 alleles of a randomly chosen European control population. At the protein level, this mutation converts a highly conserved arginine 729 (Fig. 1B) into a tryptophan residue (p.R729W).

Sequencing of the parental DNA confirmed the father as being heterozygous for this mutation, whereas the mother only presented the normal sequence (Fig. 1A). A *de novo* mutation on the maternal allele was excluded by the identification of two single nucleotide polymorphisms (SNPs), in exon 5 and exon 18, which also showed an abnormal inheritance pattern, i.e. the patient having no obvious maternal contribution for the *COG4* allele (data not shown). A uniparental paternal isodisomy of (a part of) chromosome 16 could also be excluded (data not shown). Fluorescence *in situ* hybridization using fosmid clones demonstrated a deletion of clone G25P85580E2, pointing to a submicroscopical deletion on the maternal allele (Fig. 1A). On the basis of the results of other fosmids, we inferred that the first two exons of the *COG4* gene are present, whereas the 3′ breakpoint should be located in a 5 kb region between intron 2 and the fifth exon. The proximal breakpoint has not been identified but, based on SNP mapping, we delineated a 47 kb region containing

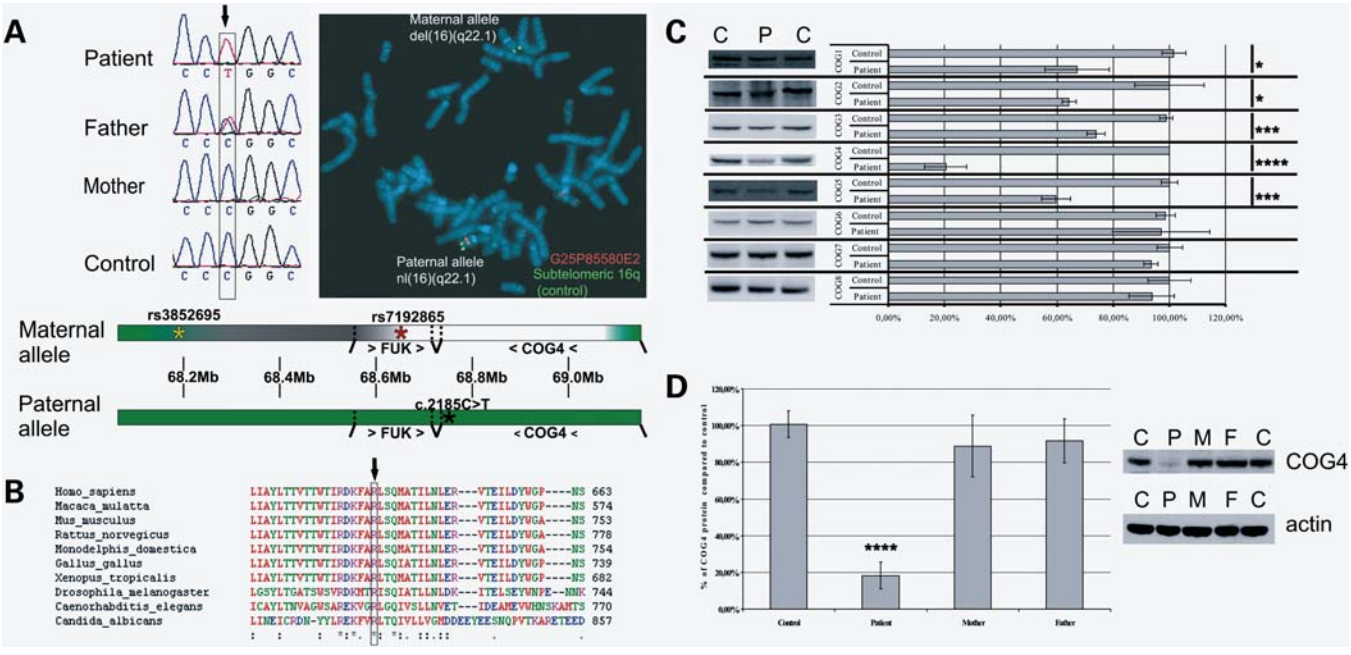

Figure 1. Genetic and molecular characterization of the described COG4 patient. (**A**) Sequencing revealed a heterozygous C>T missense mutation in the patient and the absence of this mutation in the mother. The fluorescence *in situ* hybridization (FISH) image shows the deletion of fosmid G24P85580E2 (red) on the maternal allele, whereas the control subtelomeric 16q fosmid (green) shows a normal signal. A schematic representation of the mutations present in the patient is given, the green and red asterisk on the maternal allele indicate, respectively, the last heterozygous SNP and the first hemizygous SNP in the patient, the black asterisk on the paternal allele indicates the position of the missense mutation, green regions indicate genes (> . . .>: sense/< . . .<: antisense/bars indicate the location of each gene) and intergenic regions that are present in the patient, the white and grey regions on the maternal allele indicate, respectively, the known deleted region and the region containing the proximal breakpoint. (**B**) Alignment of the COG4 sequence of different species shows an absolute conservation of this residue. (**C**) Lysates of a control, the COG4 patient and both parents were loaded on SDS–PAGE gel to analyze the COG4 levels. Quantifications represent the mean values of three independent loadings of independent samples. Error bars represent the SEM, a Student *t*-test resulted in a highly significant *P*-value (≤0.001—indicated as ****) when comparing control and patient. (**D**) Western blot of control and patient for all COG subunits. Quantifications represent the mean values of three independent loadings of independent samples. Error bars represent the SEM, a Student *t*-test was used to obtain the *P*-values indicated in the graph as */***/****, representing, respectively, $P \leq 0.1/P \leq 0.01/P \leq 0.001$.

the deletion breakpoint. The closest SNP with a normal biparental inheritance pattern was rs3852695, located 97 kb upstream of the COG4 start codon, whereas rs7192865 was the first hemizygous SNP, located 50 kb upstream of COG4 (Fig. 1A). The only other gene (largely) included in the deletion is the *FUK* gene, just upstream of the *COG4* gene. This gene encodes the L-fucose kinase, necessary for the reutilization of fucose after the degradation of oligosaccharides (22). Since no decreased fucosylation was observed in the *N*-glycans of our patient, we conclude that the (partial) monosomy of this gene is not pathogenic. In our opinion, the *COG4* deletion and point mutation are the sole responsible for the identified clinical and cellular abnormalities. This mutation defines a new subtype of CDG-II, which we named the COG4 defect (COG4/CDG) or CDG-IIj.

The patient described here is the first child of healthy, unrelated Portuguese parents. Until the fourth month the boy had a normal development, but after a vaccination the child started fever and progressive irritability. He was hospitalized due to complex seizures, which were eventually suppressed by phenobarbital. Some dysmorphic features were noted, like a peculiar face (down sloping frontal area and thick hair) combined with axial hyponia, slight peripheral hypertonia and hyperreflexia. Blood tests revealed increased serum transaminases, alkaline phosphatases and LDH cholesterol levels, while the platelet counts were down. Because CDG was suspected, isoelectric focusing of serum transferrin was performed and showed a type 2 pattern (Supplementary Material, Fig. S1). Brain MRI, ophtamological and cardiological investigations were normal, as well as serum immunoglobulins and hormones, but a decrease of coagulation factors was noted. Since the age of 12 months he was regularly admitted to the hospital due to recurrent respiratory infections. At the age of 3 years the child presented with microcephaly, bilateral cerebral atrophy of the frontotemporal regions, a mild degree of ataxia, brisk, uncoordinated movements, absence of speech and moderate psychomotor delay.

COG subcomplexes reside in the cytosol

The combination of both the mutant *COG4* and the deleted allele has a dramatic effect on COG4 protein levels that drop to 20% in the patient's fibroblasts compared with control (Fig. 1C). Interestingly, the low COG4 levels also affected the other subunits of lobe A by 50% for COG3, 40% for COG2 and 25% for COG1. In lobe B only a 40% decrease was observed for COG5, whereas all others remained indistinguishable from the control. We can thus conclude that the *COG4* mutation mainly renders lobe A subunits instable without affecting dramatically (except for COG5) lobe B subunits. Western blot analysis for COG4 on extracts derived from maternal and paternal fibroblasts displayed normal

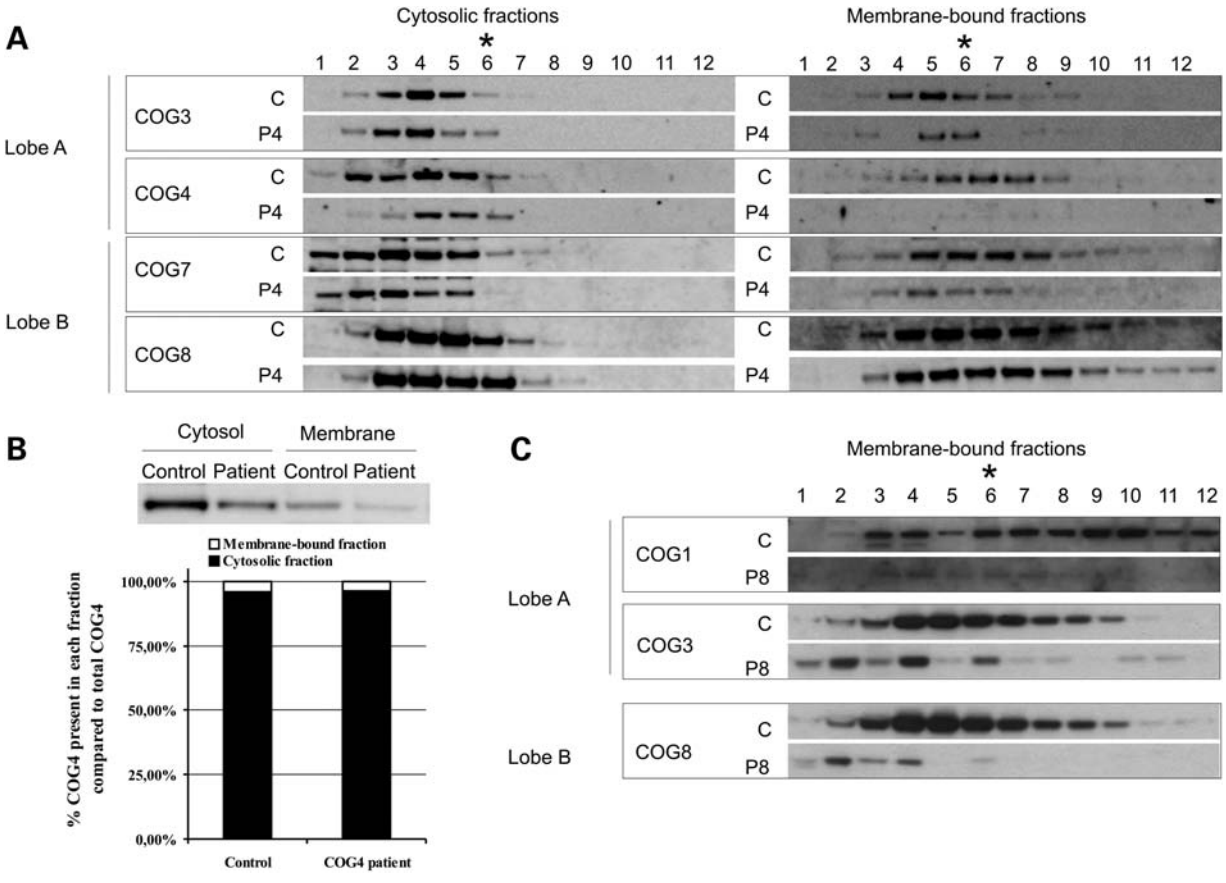

Figure 2. The COG4 mutation does not abrogate normal assembly of the full complex. (**A**) Glycerol gradient centrifugation was performed on cytosolic and membrane fractions of a control (**C**) and the COG4 patient (P4), all 12 fractions obtained were loaded onto SDS–PAGE gels and the distribution of COG3, -4, -7 and -8 was analyzed using western blot, asterisks indicate the migration of the 669 kDa marker thyroglobulin. Exposure times differ between cytosolic and membrane fractions, due to the mainly cytosolic localization of the complex. (**B**) Cytosol and membrane fractions were obtained from the cells of a control and the COG4 patient. Quantifications after western blot shows that there is no difference between the COG4 distribution in control and patient's cells. (**C**) Glycerol gradient centrifugation was performed on membrane fractions of a control (C) and the COG8 patient (P8), all 12 fractions obtained were loaded onto SDS–PAGE gels and the distribution of the COG1, -3 and -8 proteins was analyzed using western blot, asterisks indicate the migration of the 669 kDa marker thyroglobulin. Exposure times differ between cytosolic and membrane fractions, due to the mainly cytosolic localization of the complex.

protein levels despite the mother being hemizygous for *COG4* (Fig. 1D). Hence, the second, normal allele likely compensates for the deletion, explaining the absence of any phenotypical abnormalities in the mother. With respect to the father, the COG4 levels are slightly affected, suggesting that the mutant COG4 is more prone to degradation.

We next explored the effect of decreased mutant COG4 levels on the integrity of the full COG complex. Cytosolic and membrane extracts of control and COG4 patient fibroblasts were fractionated by glycerol gradient centrifugation and analyzed by western blotting. No apparent differences in the size distribution of the COG complexes were noticed when compared with control cytosolic and membrane fractions (Fig. 2A). This demonstrates that, despite the mutant COG4 and lowered levels of several individual COG subunits, complexes can still be formed. This contrasts with the observations made for the COG8-deficient patient (12). On the other hand, we observed clear differences between cytosolic and membrane extracts with COG complexes distributing in much lighter fractions of the cytosolic gradients and in a more restricted manner (fractions 2–6). In comparison, the 669 kDa marker thyroglobulin was recovered mainly in fraction 6. In the case of membrane extracts, COG subunits were more broadly distributed and found in higher fractions as well. Moreover, when comparing the absolute amounts of cytosolic and membrane-associated COG subunits, most is recovered in the cytosol (Fig. 2B). Taken together, these results suggest that the full complex, with an estimated weight of ~800 kDa, is mainly present on the membrane. The broad distribution of the COG proteins in the membrane gradients indicates that both the full complex and subcomplexes coexist in the membrane. The cytosol contains the major pool of COG proteins, but mainly in the form of subcomplexes, probably corresponding to lobe A and B. In the light of this, it is tempting to suggest that subcomplexes present on the vesicle and target membrane recombine to full COG complexes upon tethering of the incoming vesicle with the Golgi membrane. Alternatively, we cannot exclude that full complexes are assembled in the cytosol and then immediately recruited to the membrane, initiating vesicle tethering (see Discussion). These results are in agreement with previous data on the COG8-deficient patient where Foulquier *et al.* (12) showed that the cytosolic COG proteins in the patient were

Table 1. Comparison of the different patients for all investigated defects

	COG1	COG4	COG7	COG8
Clinical phenotype	Failure to thrive Hypotonia	Mild psychomotor retardation	Lethal Growth retardation	Encephalopathy Neurological and psychomotor regression
	Mild psychomotor retardation	Mild dysmorphia	Dysmorphia	Hypotonia
	Growth retardation	Epilepsia	Hyperthermia	Mild mental retardation
Mutation(s)	c.2659-2660insC p.P888fsX900	c.2185C>T p.R729W submicroscopical deletion 16q22	c.IVS1+4A>C altered splicing leading to frame shift and stop codon	c.1611C>G p.Y537X
Origin	Portuguese	Portuguese	Moroccan	Spanish
Publication	Foulquier *et al*. (15)	This publication	Wopereis *et al*. (17)	Foulquier *et al*. (12)
BFA defect (% cells with Golgi remnants)	74.6 ± 2.5	22 ± 3.5	88.8 ± 2.33	34.4 ± 7.9
Glycosylation defects	Sialylation Galactosylation Demannosylation	Sialylation (Galactosylation)	Sialylation Galactosylation Demannosylation	Sialylation Galactosylation
Golgi morphology	Typical Golgi stacks (as in WT)	Typical Golgi stacks (as in WT)	Many undulated Golgi stacks with many swollen cisternae	Some undulated Golgi stacks
	Some undulated Golgi stacks	Some undulated Golgi stacks, less rigid	Less rigid Golgi stacks	Fragmented Golgi
	Few fragmented/ disrupted Golgi.	Few fragmented/disrupted Golgi		Many tubular and vesicular profiles

present in lighter fractions when compared with the control. When extending this analysis to the membrane fractions of the COG8 patient's fibroblasts in this study, we also noticed a more restricted distribution towards lighter fractions in accordance with the lack of full COG complex assembly on the membrane in COG8 patient fibroblasts (Fig. 2C). Upon comparison of the percentage of the COG3, -4, -7 and -8 proteins in the different fractions, the complexes in the cytosol appear definitely smaller, whereby only the COG8 patient showed a defect in full complex formation (Supplementary Material, Fig. S2). These data seem to be in disagreement with the reports on yeast and CHO cells, reporting the presence of the majority of the COG proteins in the full complex (13,23–27). However, we feel caution is needed when extrapolating experiments from different organisms to primary human fibroblasts, since differences in the mechanism of the formation of the full complex cannot be excluded.

At the endogenous level, all COG subunits show a preferential localization to the Golgi region as demonstrated by the colocalization with GM130, a *cis*-Golgi marker. Similar observations were made in the COG4 patient's fibroblasts where all COG proteins localized to the Golgi (Supplementary Material, Fig. S3), in spite of the very low levels of mutant COG4 (and other subunits) in these cells. The absence of a significantly different localization could be due to the large cytosolic pool from which subcomplexes can be recruited. These and previous findings suggest that the mutation in COG4 generates a more subtle effect in the COG complex function, for instance by affecting recruitment of other regulatory components in membrane tethering.

The degree of Golgi dysfunction grossly correlates with the clinical phenotype

Next we compared this patient with three patients harbouring mutations in COG1, COG7 or COG8 (12,15,17) on multiple parameters. With respect to the clinical phenotypes (Table 1 and Supplementary Material, Table S1), it is evident that the COG7 patient is most affected. Also the clinical phenotype of the COG8 patient is quite severe, whereas the COG4 and mainly the COG1 patients present with milder problems. The question now rises whether this correlates with the defects observed at the cellular level.

The initial classification of patients with mutations in COG subunits as CDG-II already identifies them with defects in the maturation of the *N*- (and *O*-) glycan chains and implicates a crucial role of the COG complex in the normal glycosylation reaction as observed also in COG subunit deficient cells (13,28). Indeed, a comparative mass-spectrometric analysis of *N*-glycans on serum samples of four COG-deficient CDG-II patients reveals multiple abnormal oligosaccharide structures and changes in the relative amounts of individual oligosaccharides. A common observation between all COG patients is the decrease in or lack of sialylation (Fig. 3A–B). With respect to this, the COG1 and COG4 patients are most, respectively least, severely affected. When comparing the galactosylation of the *N*-glycans, both COG1 and COG7 patients were most affected with agalactosylated glycan structures in, respectively, 11 and 40% of the glycans. This result was striking since in the described CDG-IId patient this defect is not observed, despite a proven 95% reduction in the β-1,4-galactosyltransferase-1 (β-1,4-GalT1) enzyme activity (29). One explanation could be that the altered recycling of the β-1,4-GalT1 enzyme, due to COG deficiencies, has a more severe effect on the formation of the correct glycan structure than a reduced β-1,4-GalT1 expression. Furthermore, only in these two patients, $Man_5GlcNAc_2$ structures were abundantly detected. The absence of a third *N*-acetylglucosamine (GlcNAc) monosaccharide is most likely due to a decreased *N*-acetylglucosaminyl transferase 1 (GlcNAcT1) activity rather than a destabilization of ManII since mannose (Man) N°6 and N°8 can only be cleaved after a GlcNAc residue is added onto the free mannose N°2 by GlcNAcT1. Both the GlcNAcT1 and ManII enzymes reside

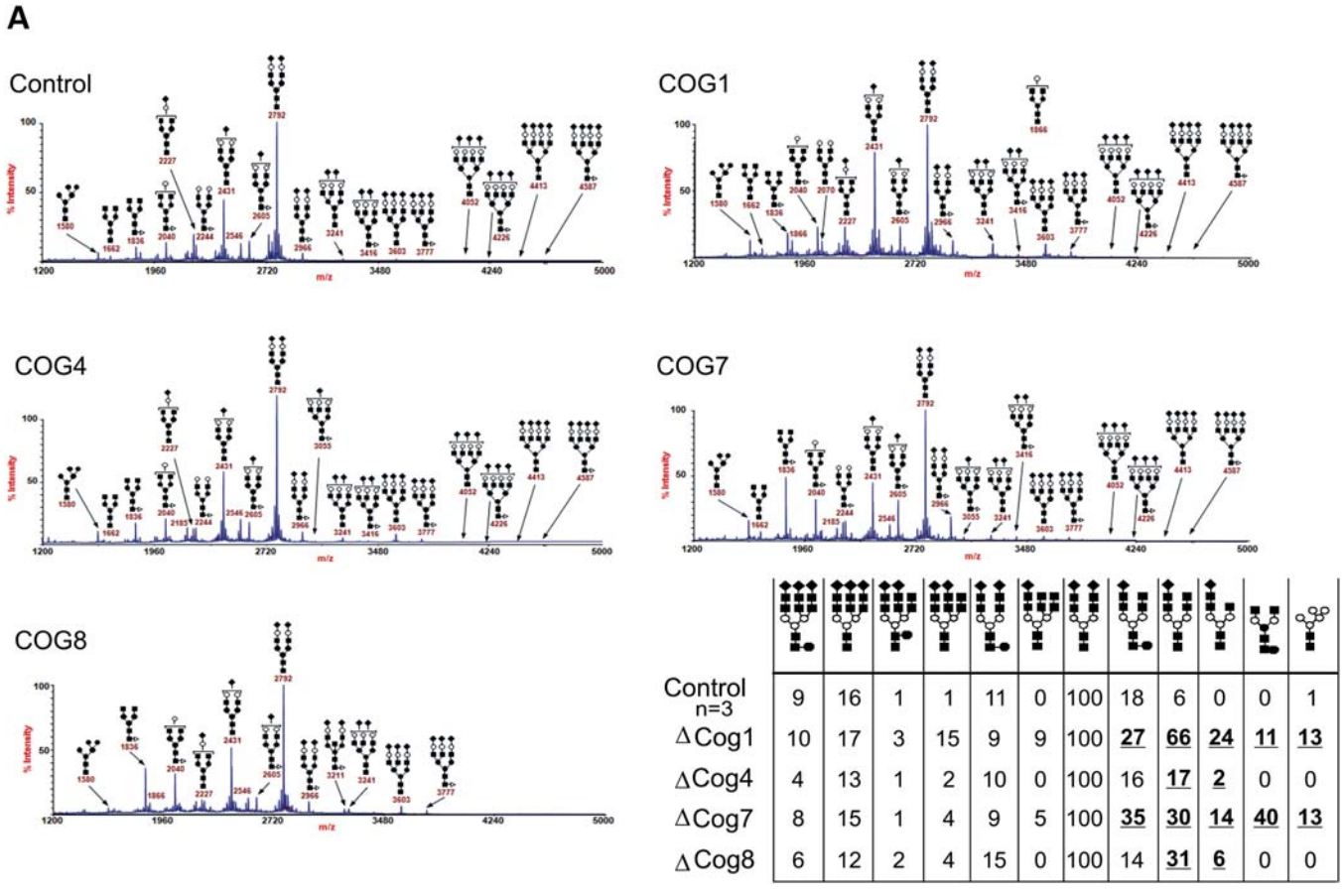

Control n=3	9	16	1	1	11	0	100	18	6	0	0	1
ΔCog1	10	17	3	15	9	9	100	**27**	**66**	**24**	**11**	**13**
ΔCog4	4	13	1	2	10	0	100	16	**17**	**2**	0	0
ΔCog7	8	15	1	4	9	5	100	**35**	**30**	**14**	**40**	**13**
ΔCog8	6	12	2	4	15	0	100	14	**31**	**6**	0	0

Figure 3. Presence of abnormal *N*-glycosylated proteins in the serum of the COG-deficient patients. (**A**) Mass spectrometry results of serum samples of all known patients and a control, show a deficiency in the *N*-glycosylation pathway in the Golgi apparatus in all patients. (**B**) Quantification of the results shown in (A), the control values are the mean of the results obtained from serum samples of three independent controls. All patients have a clear decrease in sialylation of their *N*-glycan chains (m/z 2431 and 2605), furthermore the COG1 and -7 patients also show a remarkable galactosylation (m/z 2040) and demannosylation (m/z 1580) deficiency.

in the same cisternae and are therefore tightly associated with one another, in order to ensure their sequential activity. Our observation is in line with earlier data on the depletion of either lobe A or lobe B of the COG complex, which severely affects localization of medial-Golgi enzymes such as GlcNAcT1 and ManII (30) and which in turn suggests a Golgi disorganization.

Even though the glycosylation defect allowed us to classify these patients as CDG-II, it is likely not the primary defect. The aberrant glycosylation may result from the abnormal transport or distribution of glycosylation enzymes and possibly also nucleotide-sugar transporters. To test the integrity of the retrograde Golgi-to-ER trafficking, we treated patient cells for 6 min with Brefeldin A (BFA), a fungal metabolite that rapidly redistributes Golgi enzymes to the ER (31–33), and counted the number of cells which still showed Golgi remnants (Fig. 4B). While in the control virtually, no cells could be detected with Golgi remnants, as measured by ManII immunoreactivity (Fig. 4A), its BFA-induced redistribution was significantly delayed in patient cells, most dramatically in COG7 and COG1 mutant cells (respectively, 90% (SEM: $\pm$2%) and 75% ($\pm$2%) of cells with Golgi remnants). A significant but less severe retrograde transport delay was observed in the COG4 and COG8 fibroblasts. The difference between COG4 and COG8 cells persisted in shorter BFA treatments but caught up with longer treatments (data not shown). On the contrary, no differences were found after 90 min of BFA wash-out, this time point was chosen since shorter incubations resulted in only a partial restoration of the Golgi in control cells (Fig. 4A) These data indicate no delay in anterograde transport and Golgi restoration in the COG-deficient patient cells.

We next attempted to rescue the BFA-induced retrograde transport defect in COG4 patient cells by introducing wild-type COG4 using retroviral transduction. BFA-treatment of these transduced cells did not result in a normalized retrograde trafficking (Fig. 5A). Surprisingly, stable transduction of control cells with COG4 (thereby doubling expression levels) resulted in a retrograde trafficking defect, reminiscent of that observed in patient cells. This indicates that COG4 overexpression leads to a dominant-negative effect on trafficking making rescue experiments very difficult. Therefore, we down-regulated COG4 in HeLa cells to try and mimic the transport defect observed in the patient's cells, by transfection of these cells with a 'smart pool' of four different RNAi oligonucleotides. This yielded a reproducible and nearly complete

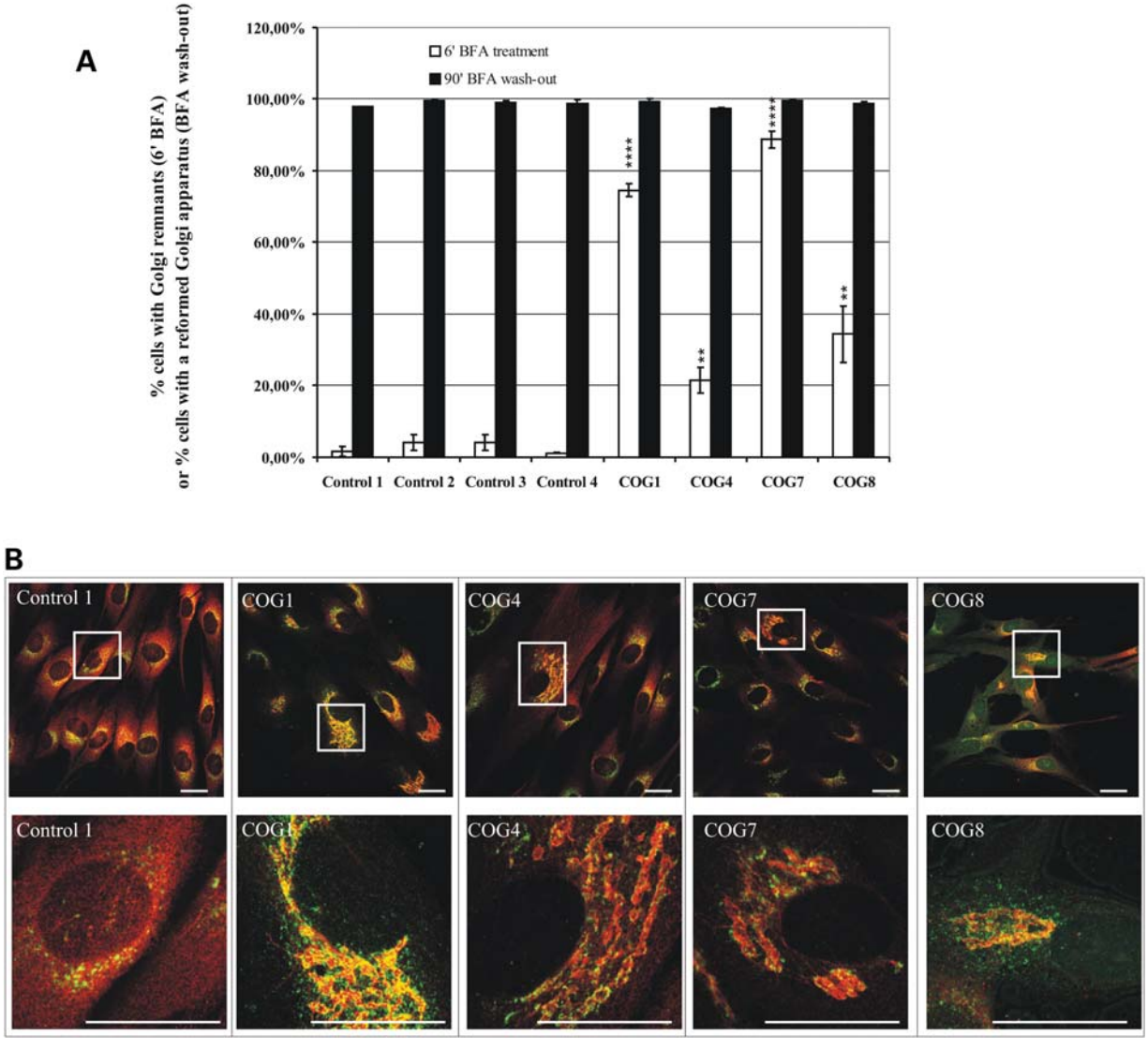

Figure 4. Cells of all known COG patients show trafficking defects. (**A**) Cells of all patients and four controls were treated with Brefeldin A for 6 or 60 min followed by wash-out of the drug. Cells were stained for GM130 and ManII, 300 cells were counted per cell line and based on the ManII staining each counted cell was scored for the presence or absence of Golgi (remnants), the results are averages of three independent experiments per cell line, the error bars represent the SEM, a Student *t*-test was used to obtain the *P*-values indicated in the graph as **/****, representing, respectively, $P \leq 0.05/P \leq 0.001$. (**B**) Representative confocal laser scanning microscopy (CLSM) images of control and patient cells obtained after staining for GM130 (green) and ManII (red). Both 60× and representative zoomed pictures are shown, scale bars represent 10 μm.

downregulation of COG4 ($3.2 \pm 3.5\%$ remaining protein) when compared with untreated or mock-transfected cells (Fig. 5B). Subsequent BFA treatment showed a significant delay in ManII re-distribution underscoring that the mutations in the patient result in a trafficking delay and are likely to be pathogenic (Fig. 5B).

Ultrastructural support for a role for the COG complex in maintaining Golgi integrity

Since Golgi integrity is maintained dynamically, we predicted that COG subunit mutations or deficiencies may alter Golgi morphology. Using confocal microscopy, we indeed noticed dilatation and fragmentation of the Golgi in all patients' cells (data not shown). However, since confocal microscopy does not give the resolution needed to observe the specific and subtle changes we decided to perform TEM analysis on all patient cells. The overall Golgi integrity was substantially to very severely disrupted in all investigated cell lines, although some distinct observations could be made (Fig. 6 and Supplementary Material, Fig. S4). First, only in COG1 and, albeit to a lesser extent, in COG4 cells few typical Golgi cisternae could still be discerned. In COG7 and COG8 patient cells on the contrary, virtually no normally organized stacks were found. In these cells, individual Golgi stacks had an undulated appearance suggesting a decreased rigidity maybe caused by a weaker connection to the underlying cytoskeleton, although this remains to be investigated. Further, fragmented or vesiculated Golgi membranes were predominantly observed in the COG8-deficient cells and less frequent

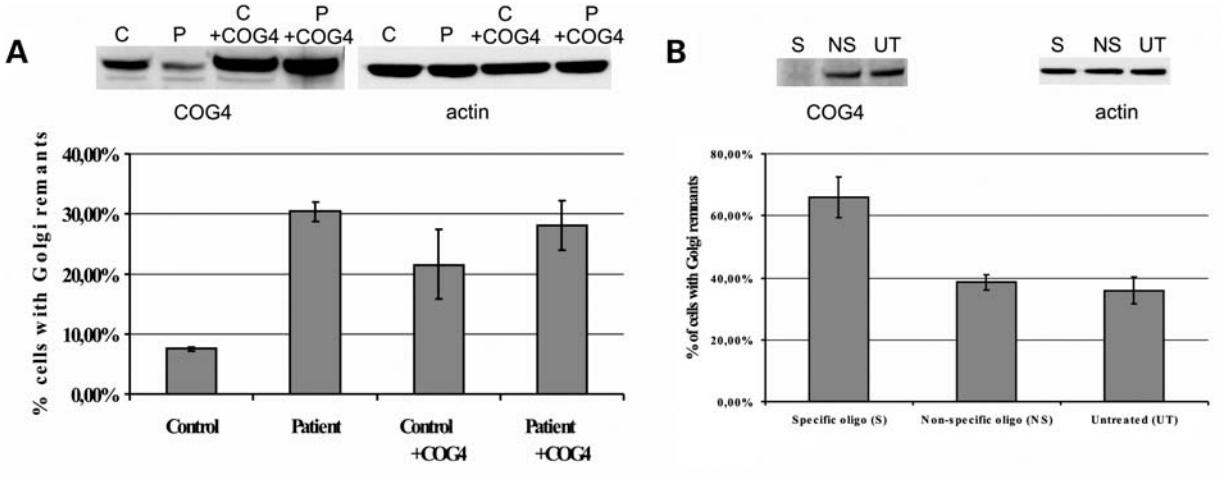

Figure 5. Effects of COG4 overexpression and downregulation on the retrograde trafficking defect. (**A**) Patient and control cells were transduced with COG4-containing viral particles, the resulting overexpression was analyzed on western blot and compared with COG4 levels present in untreated control and patient cells. After BFA treatment of all four cell lines the percentage of abnormal cells was counted, based on ManII staining, results are averages of three independent BFA treatments, error bars represent the SEM. (**B**) HeLa cells were transfected three times independently with a 'smart pool' of RNAi oligo's specific for the COG4 sequence (S). The extent of downregulation was assessed using western blot and compared with untreated cells (UT) and cells treated with a non-specific oligo (NS). The percentage of abnormal cells, counted after BFA treatment and ManII staining, is represented in the graph as an average of three different experiments. Error bars represent the SEM, a Student *t*-test was performed resulting in a significant *P*-value of 0.022, when compared with the untreated cells.

in COG4 and COG1 cells. Fragmentation was not clearly observed in the COG7 cells but instead the Golgi areas presented with many individual swollen cisternae (asterisk in Fig. 6). Such swollen cisternae were also frequently seen in COG8 cells. It should be noticed that at the EM level many COG7 patient cells appeared necrotic indicating that the observed ultrastructural defects in the surviving cells are an underestimation of the true phenotype. Again, a correlation can be found between the severity of the disease and the corresponding ultrastructural defects. Surprisingly, however, and in spite of having severe structural deficits in Golgi integrity and transport, patient cells still maintain a significant degree of complex glycosylation.

DISCUSSION

Clinical comparison of different COG-deficient CDG-II patients

The present study identifies a novel mutation in the COG4 subunit of the COG complex (designated as CDG-IIj), which further expands the subgroup of CDG-II cases caused by mutations in the COG complex (12,14–19). Thus far, mutations have been detected in the COG1, COG7 and COG8 subunits and range from premature stop codons in the COG1 and COG8 to splice site mutations in the COG1 and COG7 subunits. Here, we describe a missense mutation combined with a microdeletion in COG4. The clinical and cellular phenotypes in these patients differ accordingly from mild to severe or lethal (Table 1 and Supplementary Material, Table S1). Herein, the COG4 phenotype is one of the mildest in this subcategory of CDG-II. Most severe are the COG7-deficient patients displaying early post-natal lethality. The overall phenotype of the COG8 patient, presenting with neurological regression, cerebellar atrophy and hypotonia, is in between that of the COG7 and COG4 patients. While the COG1 mutation causes an early stop codon and hence a large C-terminal truncation, the patient suffers only from mild psychomotor retardation.

Effects of the p.R729W COG4 mutation on complex formation and its function

The COG4 patient is compound heterozygous for a R729W point mutation and a submicroscopical deletion. In heterozygous state, the individual gene defects do not compromise COG function given the absence of clinical features in both parents. The combination, however, results in 20% reduced levels of the mutant COG4 subunit and consequently, the levels of the corresponding lobe A subunits are also significantly reduced, a feature reminiscent of COG mutations (12,14–19). Unexpectedly, a significant drop in COG5, a lobe B subunit, was observed suggesting interaction of COG5 with lobe A (subunits). In support, COG5 was demonstrated *in vitro* to interact with COG4 (11) as well as with COG1 (27). Nevertheless, the remaining mutant COG4 protein retains its capacity to integrate in an octameric COG complex as demonstrated by glycerol gradient centrifugation. This also implies that the destabilized COG1, which bridges both lobes through its interaction with COG8, is still present in sufficient amounts for complex formation (12,24). Our data therefore suggest the existence of a pool of subunits or subcomplexes from which full complexes can be assembled according to the cellular needs. Hence in the COG4 patient cells, the reduced lobe A levels are apparently sufficient to maintain a basal level of COG complex formation. Indeed, the fact that over 90% of the COG proteins are cytosolic and mostly distributing in the lighter fractions of the gradient suggests that they are predominantly associated in their lobe A or B configuration. On the other hand, when analyzing

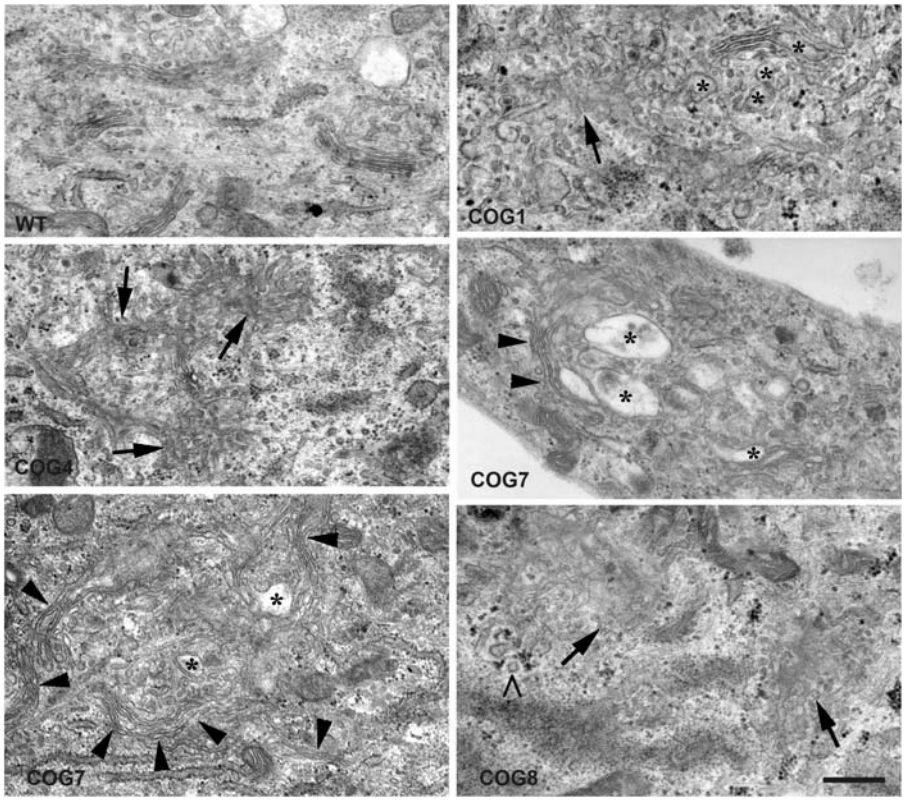

Figure 6. Analysis of the Golgi morphology at the submicroscopical level. Cells of all patients and one control were subjected to electron microscopy. Both the COG1- and COG4-deficient patient cells still show some stacks with a normal morphology, in contrast to the COG7 and COG8 patients. The most striking finding mainly in the COG7 and COG8 patients was the undulated appearance of the stacked cisternae, as indicated by the arrowheads. Furthermore, several stacks have a fragmented and/or vesiculated appearance, indicated by arrows, a phenotype which is most severe in the COG8 patient. The asterisks indicate swollen cisternae which were present in a differing degree in all patients. The '>'points to clathrin-coated vesicles, indicating the *trans*-side of the Golgi apparatus.

membrane extracts, most subunits are trailing broadly over almost the complete gradient suggesting an additional association in higher order complexes, likely the full COG complex. The observation that mutant COG8 membrane extracts (in which the lobe A and B bridging is disrupted) lack this trailing indicates that in this case only (partial) subcomplexes are membrane bound. In the light of these data, it is tempting to suggest two possible mechanisms in which the COG complex could tether incoming vesicles. First, lobe A and B might be recruited to the membrane of either the incoming vesicle or the target (Golgi cisternal) membrane. When in close proximity, both lobes can combine to a full complex thereby tethering the transport vesicle to the cisterna. After fusion, the full complex dissociates from the membrane and into subcomplexes (Fig. 7A). This model is in agreement with the proposed working mechanism of the exocyst complex at the cell surface. It has been reported that the Sec3p and Exo70p exocyst subunits localize to the target membrane, whereas the others are recruited to the vesicle and full complex formation assists tethering (34). On the other hand, and in analogy to the TRAPP complex (34), all eight subunits might assemble in the cytosol and be recruited to either the vesicular or target membrane and assist tethering after capture of the vesicle by other proteins, such as p115 for which an interaction with COG2 has been demonstrated (35) (Fig.7B). However, giving the striking similarity in the sequence and structure between subunits of the exocyst and COG complex (36,37, Richardson *et al*., manuscript in preparation), the first model is favoured here. Whether the recruitment of both lobes, or the full complex occurs directly through lipid interactions or via yet to be identified membrane proteins on the vesicle and/or cisternal membrane remains to be explored.

The presence of a major cytosolic reserve pool is supported by immunolocalization studies that showed no significant alterations in the Golgi association of the mutant COG4 or other COG subunits. Only in more dramatic cases, such as in the human fibroblasts deficient in COG 1, COG7 or COG8 (12,14,15) but also after knock-down of COG2, COG3 or COG5 (28,38), the steady-state localization of some of the cognate subunits was affected; this is likely due to the abrogation of inter-subunit interactions caused by e.g. the truncation or destabilization of the COG1 and/or COG8 proteins.

Cellular implications of single COG subunit deficiencies

At the cellular level, all COG mutations display a significant mild to severe delay in BFA-induced redistribution of Golgi enzymes (as evidenced by mannosidase II) or Golgi matrix

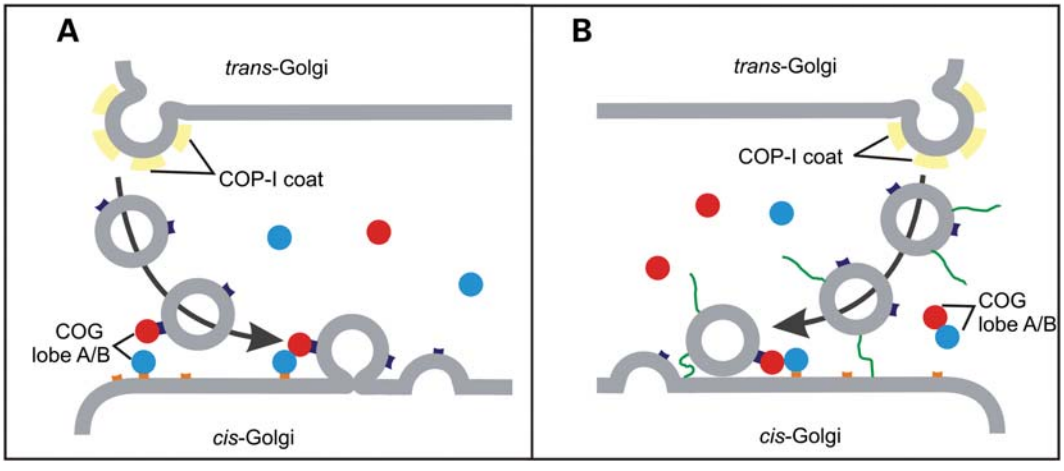

Figure 7. Hypothetical models on (the regulation of) the action of the COG complex. Retrograde transport organelles as well as target antecedent cisternal membranes are proposed to recruit single lobe A or B subcomplexes (red and blue circles) from cytosolic pools. Tethering of the vesicle to the cisternal membrane occurs by binding of both lobes and full complex formation (**A**) or by directly binding of the full complex to either of the membranes (**B**). Recruitment of the COG complex to the membrane may include, as yet unknown, proteins (orange and purple boxes). Also, model B suggests the presence of a long-distance tether (green line) that initially captures the vesicle prior to COG complex recruitment. After tethering, the soluble NSF attachment protein receptor (SNARE) fusion machinery drives the fusion of vesicle and membrane followed by dissociation of the COG complex from the membrane and from each other.

proteins (such as GM130) to the ER, ER exit sites or perinuclear vesicular structures (32,39,40). The lack of any effect in BFA wash-out experiments clearly indicates a retrograde transport defect and a putative role for the COG complex in tethering retrograde transport vesicles to the antecedent cisternae as predicted by the cisternal maturation model (8,9,41–43). Any defect in retrograde intra-Golgi trafficking and tethering is likely to affect Golgi morphology due to imbalanced transport of e.g. cargo. Indeed ultrastructural analysis revealed abundant Golgi fragmentation, vesiculation and cisternal vacuolization in all mutant COG fibroblasts largely correlating with the severity of the mutations and the observed delays in BFA-induced redistributions. In agreement, overall Golgi fragmentation, often associated with vacuolated cisternae, was observed for the ldlB and ldlC mutant CHO cells, deficient in either COG1 or COG2 (13,44). Downregulation of COG3 resulted in the formation of Golgi mini-stacks and an extensive accumulation of small vesicles distinct from COPI-coated vesicles (38), whereas knockdown of COG5 in CHO cells showed dilated Golgi cisternae (45). Finally, mutants of the yeast COG4 homologue, Sgf1, showed an accumulation of membranes, most likely Golgi transport vesicles (46). These findings underscore our findings that a deficiency in a given COG subunit substantially affects Golgi integrity. On the other hand, we also observed unexpected and novel alterations of the Golgi morphology including the presence of undulated cisternae (e.g. in COG7 and COG8 patients' cells). This points to a destabilization in the connection of the Golgi cisternae with the underlying cytoskeleton and suggests, besides a role in retrograde transport, an additional function of the COG complex (or one or more of its subunits) in tethering Golgi membranes to microtubules.

Given their Golgi localization, the observed defects in Golgi transport and morphology, COG subunit mutations are prone to affect the Golgi glycosylation processes. Still, this is the first study in its kind to analytically compare such Golgi glycosylation defects between the mutant COG subunits. Mass spectroscopical analysis of total serum *N*-glycans revealed an overall decrease in sialylation and galactosylation in all patients. Strong differences in the relative amounts of oligosaccharides and the presence of unexpected oligosaccharide structures were observed according to the affected COG subunits. Most striking was the presence of a $Man_5GlcNAc_2$ structure in COG1 and COG7 patients, suggesting an abnormal localization and/or activity of GlcNAcT1. In previous studies also a destabilization of ManII and β-1,4-GalT1 was noticed in the COG1 patient, likely explaining the observed demannosylation and galactosylation defects. On the other hand, the COG8 patient only showed a destabilization of β-1,4-GalT1 resulting in a decreased galactosylation (12,15). We can, however, not exclude that all observed glycosylation defects are caused by mislocalization of the classical glycosylation enzymes. Indeed, proper glycosylation is also crucially dependent on nucleotide-sugar transporters and mislocalization or degradation of such transporters would affect Golgi glycosylation.

There is a strong correlation between the severities of the trafficking and glycosylation abnormalities in all patients' cell lines. Hence it is likely that the deficiency in tethering of intra-Golgi retrograde vesicles impairs recycling of the responsible enzymes and/or nucleotide-sugar transporters back to their correct cisternae. Given the defects in COG function and their, mostly dramatic, effects on intra-Golgi transport and Golgi integrity, one wonders how such cells still manage to generate a vast percentage of normal oligosaccharide chains. After all, even the clinically and cellularly most severe COG7 mutation succeeds partially in this task (Fig. 3A and B). On the other hand, clinically less severe cases such as the COG1 patient have more pronounced glycosylation defects compared with others. All this suggests a high degree of plasticity of the Golgi apparatus to maintain minimal function even when structurally affected. Given the heavily disorganized or even residual appearance of Golgi complexes in the different COG mutants and mostly the lack of recognizable

cisternal organization, this plasticity is difficult to explain only on the basis of the 'cisternal maturation' model. Keeping a minimal fidelity in glycosylation could, however, be explained by the Golgi apparatus being a two-phase membrane system (10). In this model, enzymes and transmembrane cargo not only rapidly partition between two lipid phases but also exchange fast among cisternae. This rapid cargo mixing upon Golgi entry and the absence of a defined transit time as predicted by this model increases the likelihood of cargo to encounter the set of enzymes required for complex glycosylation. One could imagine that even in severely disorganized Golgi complexes such a system could support minimal glycosylation processes as observed in the different COG patients. Although speculative for the moment, cells harbouring mutant COG subunits have the potency to provide the litmus test for this provocative model on intra-Golgi transport.

Concluding remarks

In conclusion, we experimentally demonstrated here that 'natural COG mutants', found in CDG-II patients, allow for a better understanding of the role of the full COG complex and of the individual subunits and subcomplexes in tethering Golgi vesicles. Moreover, we also highlighted the important contribution of characterizing clinical mutations in the molecular and cell biological understanding of Golgi dynamics and its associated functions permitting to propose novel mechanisms or testing existing models. The predominance of COG mutations as a possible cause of CDG-II also predicts that within the growing pool of unresolved cases, likely more candidate genes will be found whose products function in intra-Golgi transport regulation.

MATERIAL AND METHODS

Cell culture and transfections

Primary fibroblasts, obtained from patients and controls, and HeLa cells were cultured in DMEM/F12 (Life Technologies, Paisley, UK), supplemented with 10% Bovine Growth Serum (HyClone, Logan, UT, USA) and were kept at 37°C in 5% CO_2.

Antibodies

Antibodies against the COG1-8 subunits were affinity purified or crude serum rabbit polyclonal antibodies. Dilutions ranged from 1 in 500 to 1 in 2000 for western blot and from 1 in 50 to 1 in 200 for confocal laser scanning microscopy imaging. Anti-COG3 pab, anti-mannosidase II pab and anti-β-1,4-GalT1 mab were gifts from, respectively, V. Lupashin (University of Arkansas for Medical Sciences, Little Rock, AR, USA), K. Moremen (University of Georgia, Athens) and E. Berger (University of Zürich, Zürich). Anti-GM130 mab was purchased from BD Biosciences (Franklin Lakes, NJ, USA).

Plasmids

COG4 cDNA (NM_015386) was cloned into the pMSCV retroviral vector (Clontech Laboratories, Mountain View, CA 94043, USA), engineered with a polylinker site, as described before (47). For the production of retrovirus, we used the packaging pVPACK-Ampho vector (Stratagene, La Jolla, CA 92037, USA).

Mass spectrometric analysis of *N*-linked glycans released from total plasma proteins

Analysis of *N*-linked glycans on plasma glycoproteins was carried out by surface-enhanced laser desorption ionization time-of-flight mass spectrometry (Ciphergen, Fremont, CA, USA) essentially as described by Mills *et al*. (48). for MALDI-TOF mass spectrometry. Analysis of acidic *N*-linked glycans was performed in negative linear ion mode. The total *N*-linked glycans from plasma proteins were released enzymatically as described by Mills *et al*. (48). The reference samples were anonymous plasma samples from patients without CDG or a lysosomal storage disease.

Preparation of cytosol and membrane fractions

Cells of control and patient were cultured in 75 cm dishes up to 90% confluency and harvested, on ice, in 1 ml of 20 mM HEPES–KOH buffer pH 7.4, supplemented with a protease inhibitor cocktail. Cells were subsequently homogenized using a ball-bearing type homogenizer. Separation of membrane and cytosol was obtained upon ultracentrifugation during 1 h at 100 000*g* at 4°C. After removal and storage of the cytosolic fractions, the pellet was dissolved in 1 ml 20 mM HEPES–KOH buffer pH 7.4 supplemented with 0.1 M NaCl and 1% CHAPS. After 1 h incubation at 4°C the insoluble material was pelleted upon ultracentrifugation at 55 000*g* during 15 min at 4°C. The membrane-containing supernatant fractions were removed and stored. The obtained samples were concentrated by $CHCl_3$/MeOH/H_2O (3/2/1) precipitation and subsequently loaded onto a 4–12% Bis-Tris SDS–PAGE pre-casted electrophoresis gel (Invitrogen, Carlsbad, CA, USA) and further processed as described in the Supplementary Material.

Glycerol gradient centrifugation

Preparation of the cytosolic and membrane fractions was identical to the protocol above. After collection, the samples were loaded onto a 12 ml 10–30% glycerol (w/v) gradient. The gradients were centrifugated in a Beckman SW40 rotor at 120 000*g* during 15 h, with slow acceleration and deceleration. Fractions of 1 ml were collected via a hole punched in the bottom of the tubes. Concentration of the samples was also done by a $CHCl_3$/MeOH/H_2O (3/2/1) precipitation, followed by loading of the resulting fractions onto a 4–12% Bis-Tris SDS–PAGE pre-casted electrophoresis gel and further processed as described in the Supplementary Material.

ER–Golgi trafficking assay

Cells were seeded onto glass coverslips in a six-well plate and allowed to grow until 75–90% confluency during 48 h. To assay the retrograde Golgi-to-ER trafficking BFA, purchased from Sigma (St Louis, MO, USA), was diluted up to 5 μg/ml in normal growth medium and this solution was pre-warmed at

37°C, before adding to the cells. Two millilitre of medium containing the drug was added per well and the cells were replaced in the incubator as soon as possible. Immediately after the end of the treatment, the plates were put on ice, the medium was taken off and 1 ml of 4% paraformaldehyde was added per well. After a 30 min fixation the coverslips were further stained for GM130 and mannosidase II, as described in the Supplementary Material.

To assay the anterograde ER-to-Golgi trafficking and the reformation of the Golgi from the ER, BFA was diluted up to 0.25 μg/ml in normal growth medium. After pre-warming the solution to 37°C, 2 ml was added per well and the cells were replaced in the incubator for 1 h. Afterwards, the coverslips were extensively washed in PBS and placed in new wells, containing fresh, BFA-free, medium. The plates were again placed in the incubator, for 90 min, after which the cells were put on ice, washed and fixed with paraformaldehyde. Again this treatment was followed by immunofluorescence staining for GM130 and mannosidase II, as described in the Supplementary Material.

Transmission electron microscopy

For TEM cells were grown in a 25 cm^2 flask and, upon reaching 95% confluency, fixed for 30 min at RT with 2% paraformaldehyde in 0.1 M phosphate buffer pH 7.4. After removal of the fixative cells were kept in 4% paraformaldehyde until processing for EPON embedding, as described previously (49) and analyzed after ultrathin sectioning.

Production of retroviral particles

Cultured 293T cells are splitted 1 over 20 before reaching 70% confluency and plated in a 15 cm dish. Upon reaching 90% of confluency the cells are transfected with the pMSCV vector and the pVPACK-Ampho plasmid (in total 20 μg) in serum-free DMEM/F12 medium (Life Technologies, Paisley, UK) and using Fugene-6 (Roche Applied Science, Indianapolis, IN, USA). The medium is replaced 24 h after transfection and 24 h later the first retroviral-containing supernatant is harvested, using a blunt-end needle and a 0.45 μm filter. In total, four harvests were obtained, with an alternating time difference of 6 and 12 h between two harvests. Obtained samples were instantly frozen in liquid nitrogen and stored at −80°C.

Transduction of fibroblasts

One day in advance cells are splitted into a six-well plate at 150 000 cells per well, in order to have a 50–70% confluency the day after. The medium is removed and 1 ml medium containing 16 μg polybrene (Sigma) and 1 ml of viral supernatant are added. After 24 h, the selection using puromycin (Sigma) is started in order to obtain a stable cell line.

SUPPLEMENTARY MATERIAL

Supplementary Material is available at *HMG* online.

ACKNOWLEDGEMENTS

We gratefully thank B. Richardson, V. Lupashin and F. Hughson for the communication of results prior to publication. This work was greatly supported through discussions with and help of Dr J. Jaeken, Dr H. Carchon, Dr R. Zeevaert and S. van Aerschot (Universitary Hospital of Leuven), Dr L. Vilarinho (Medical Genetics Institute, Porto), Dr J. Vermeesch, Dr T. Voet, Dr G. Froyen, L. Keldermans, W. Vleugels, R. Thoelen (Center for Human Genetics, Leuven) and D. Xanthakis (University Medical Center Utrecht). We are grateful to Dr K. Moremen, Dr E.G. Berger and Dr V. Lupashin for kindly providing us with antibodies.

Conflict of Interest statement. None declared.

FUNDING

This work was supported by an 'Instituut voor de Aanmoediging van Innovatie door Wetenschap en Technologie Vlaanderen' (IWT) scholarship [grant number SB53523] to E.R.; a 'Fonds voor Wetenschappelijk Onderzoek Vlaanderen' (FWO) grant to W.A. [grant number G.0504.06] and G.M. [grant number G.0553.08]; a Marie Curie European Reintegration Grant to F.F.; the 'Vlaams Instituut voor Biotechnologie' (VIB) (to W.A.); the 'Katholieke Universiteit Leuven' (to W.A. and G.M.) and the Sixth Framework program of the European Union [Euroglycanet grant number: LSHM-2005-512131] (to G.M.). Funding to pay the Open Access publication Charges for this article was provided by a 'Fonds voor Wetenschappelijk Onderzoek Vlaanderen' (FWO) grant to W.A. [Grant number G.0504.06].

REFERENCES

1. Lippincott-Schwartz, J. and Zaal, K.J. (2000) Cell cycle maintenance and biogenesis of the Golgi complex. *Histochem. Cell Biol.*, **114**, 93–103.
2. Yan, A. and Lennarz, W.J. Unraveling the mechanism of protein *N*-glycosylation. *J. Biol. Chem.*, **280**, 3121–3124.
3. Holthuis, J.C., Pomorski, T., Raggers, R.J., Sprong, H. and Van Meer, G. (2001) The organizing potential of sphingolipids in intracellular membrane transport. *Physiol. Rev.*, **81**, 1689–1723.
4. Dunphy, W.G. and Rothman, J.E. (1985) Compartmental organization of the Golgi stack. *Cell*, **42**, 13–21.
5. Rothman, J.E., Miller, R.L. and Urbani, L.J. (1984) Intercompartmental transport in the Golgi complex is a dissociative process: facile transfer of membrane protein between two Golgi populations. *J. Cell Biol.*, **99**, 260–271.
6. Bretscher, M.S. and Munro, S. (1993) Cholesterol and the Golgi apparatus. *Science*, **261**, 1280–1281.
7. Nilsson, T. and Warren, G. (1994) Retention and retrieval in the endoplasmic reticulum and the Golgi apparatus. *Curr. Opin. Cell Biol.*, **6**, 517–521.
8. Glick, B.S., Elston, T. and Oster, G. (1997) A cisternal maturation mechanism can explain the asymmetry of the Golgi stack. *FEBS Lett.*, **414**, 177–181.
9. Puthenveedu, M.A. and Linstedt, A.D. (2005) Subcompartmentalizing the Golgi apparatus. *Curr. Opin. Cell Biol.*, **17**, 369–375.
10. Patterson, G.H., Hirschberg, K., Polishchuk, R.S., Gerlich, D., Phair, R.D. and Lippincott-Schwartz, J. (2008) Transport through the Golgi apparatus by rapid partitioning within a two-phase membrane system. *Cell*, **133**, 1055–1067.
11. Ungar, D., Oka, T., Vasile, E., Krieger, M. and Hughson, F.M. (2005) Subunit architecture of the conserved oligomeric Golgi complex. *J. Biol. Chem.*, **280**, 32729–32735.

12. Foulquier, F., Ungar, D., Reynders, E., Zeevaert, R., Mills, P., Garcia-Silva, M.T., Briones, P., Winchester, B., Morelle, W., Krieger, M. *et al.* (2007) A new inborn error of glycosylation due to a Cog8 deficiency reveals a critical role for the Cog1–Cog8 interaction in COG complex formation. *Hum. Mol. Genet.*, **16**, 717–730.
13. Ungar, D., Oka, T., Brittle, E.E., Vasile, E., Lupashin, V.V., Chatterton, J.E., Heuser, J.E., Krieger, M. and Waters, M.G. (2002) Characterization of a mammalian Golgi-localized protein complex, COG, that is required for normal Golgi morphology and function. *J. Cell Biol.*, **157**, 405–415. Epub 2002 April 29.
14. Wu, X., Steet, R.A., Bohorov, O., Bakker, J., Newell, J., Krieger, M., Spaapen, L., Kornfeld, S. and Freeze, H.H. (2004) Mutation of the COG complex subunit gene COG7 causes a lethal congenital disorder. *Nat. Med.*, **10**, 518–523. Epub 2004 April 25.
15. Foulquier, F., Vasile, E., Schollen, E., Callewaert, N., Raemaekers, T., Quelhas, D., Jaeken, J., Mills, P., Winchester, B., Krieger, M. *et al.* (2006) Conserved oligomeric Golgi complex subunit 1 deficiency reveals a previously uncharacterized congenital disorder of glycosylation type II. *Proc. Natl Acad. Sci. USA*, **103**, 3764–3769. Epub 2006 February 28.
16. Kranz, C., Ng, B.G., Sun, L., Sharma, V., Eklund, E.A., Miura, Y., Ungar, D., Lupashin, V., Winkel, D.R., Cipollo, J.F. *et al.* (2007) COG8 deficiency causes new congenital disorder of glycosylation type IIh. *Hum. Mol. Genet.*, **16**, 731–741.
17. Morava, E., Zeevaert, R., Korsch, E., Huijben, K., Wopereis, S., Matthijs, G., Keymolen, K., Lefeber, D.J., De Meirleir, L. and Wevers, R.A. (2007) A common mutation in the *COG7* gene with a consistent phenotype including microcephaly, adducted thumbs, growth retardation, VSD and episodes of hyperthermia. *Eur. J. Hum. Genet.*, **15**, 638–645.
18. Ng, B.G., Kranz, C., Hagebeuk, E.E., Duran, M., Abeling, N.G., Wuyts, B., Ungar, D., Lupashin, V., Hartdorff, C.M., Poll-The, B.T. *et al.* (2007) Molecular and clinical characterization of a Moroccan Cog7 deficient patient. *Mol. Genet. Metab.*, **91**, 201–204.
19. Zeevaert, R., Foulquier, F., Dimitrov, B., Reynders, E., Van Damme-Lombaerts, R., Simeonov, E., Annaert, W., Matthijs, G. and Jaeken, J. (2008) Cerebrocostomandibular-like syndrome and a mutation in the conserved oligomeric Golgi complex, subunit 1. *Hum. Mol. Genet.*, **18**, 517–524.
20. Grunewald, S., Matthijs, G. and Jaeken, J. (2002) Congenital disorders of glycosylation: a review. *Pediatr. Res.*, **52**, 618–624.
21. Jaeken, J. (2003) Komrower lecture. Congenital disorders of glycosylation (CDG): it's all in it!. *J. Inherit. Metab. Dis.*, **26**, 99–118.
22. Hinderlich, S., Berger, M., Blume, A., Chen, H., Ghaderi, D. and Bauer, C. (2002) Identification of human L-fucose kinase amino acid sequence. *Biochem. Biophys. Res. Commun.*, **294**, 650–654.
23. Walter, D.M., Paul, K.S. and Waters, M.G. (1998) Purification and characterization of a novel 13 S hetero-oligomeric protein complex that stimulates *in vitro* Golgi transport. *J. Biol. Chem.*, **273**, 29565–29576.
24. Chatterton, J.E., Hirsch, D., Schwartz, J.J., Bickel, P.E., Rosenberg, R.D., Lodish, H.F. and Krieger, M. (1999) Expression cloning of LDLB, a gene essential for normal Golgi function and assembly of the ldlCp complex. *Proc. Natl Acad. Sci. USA*, **96**, 915–920.
25. Kim, D.W., Sacher, M., Scarpa, A., Quinn, A.M. and Ferro-Novick, S. (1999) High-copy suppressor analysis reveals a physical interaction between Sec34p and Sec35p, a protein implicated in vesicle docking. *Mol. Biol. Cell*, **10**, 3317–3329.
26. Ram, R.J., Li, B. and Kaiser, C.A. (2002) Identification of Sec36p, Sec37p, and Sec38p: components of yeast complex that contains Sec34p and Sec35p. *Mol. Biol. Cell*, **13**, 1484–1500.
27. Fotso, P., Koryakina, Y., Pavliv, O., Tsiomenko, A.B. and Lupashin, V.V. (2005) Cog1p plays a central role in the organization of the yeast conserved oligomeric Golgi complex. *J. Biol. Chem.*, **280**, 27613–27623. Epub 2005 June 2.
28. Podos, S.D., Reddy, P., Ashkenas, J. and Krieger, M. (1994) LDLC encodes a brefeldin A-sensitive, peripheral Golgi protein required for normal Golgi function. *J. Cell. Biol.*, **127**, 679–691.
29. Hansske, B., Thiel, C., Lubke, T., Hasilik, M., Honing, S., Peters, V., Heidemann, P.H., Hoffmann, G.F., Berger, E.G., von Figura, K. *et al.* (2002) Deficiency of UDP-galactose:*N*-acetylglucosamine beta-1,4-galactosyltransferase I causes the congenital disorder of glycosylation type IId. *J. Clin. Invest.*, **109**, 725–733.
30. Shestakova, A., Zolov, S. and Lupashin, V. (2006) COG complex-mediated recycling of Golgi glycosyltransferases is essential for normal protein glycosylation. *Traffic*, **7**, 191–204.
31. Lippincott-Schwartz, J., Yuan, L.C., Bonifacino, J.S. and Klausner, R.D. (1989) Rapid redistribution of Golgi proteins into the ER in cells treated with brefeldin A: evidence for membrane cycling from Golgi to ER. *Cell*, **56**, 801–813.
32. Lippincott-Schwartz, J., Donaldson, J.G., Schweizer, A., Berger, E.G., Hauri, H.P., Yuan, L.C. and Klausner, R.D. (1990) Microtubule-dependent retrograde transport of proteins into the ER in the presence of brefeldin A suggests an ER recycling pathway. *Cell*, **60**, 821–836.
33. Chardin, P. and McCormick, F. (1999) Brefeldin A: the advantage of being uncompetitive. *Cell*, **97**, 153–155.
34. Kummel, D. and Heinemann, U. (2008) Diversity in structure and function of tethering complexes: evidence for different mechanisms in vesicular transport regulation. *Curr. Protein Pept. Sci.*, **9**, 197–209.
35. Sohda, M., Misumi, Y., Yoshimura, S., Nakamura, N., Fusano, T., Ogata, S., Sakisaka, S. and Ikehara, Y. (2007) The interaction of two tethering factors, p115 and COG complex, is required for Golgi integrity. *Traffic*, **8**, 270–284.
36. Cavanaugh, L.F., Chen, X., Richardson, B.C., Ungar, D., Pelczer, I., Rizo, J. and Hughson, F.M. (2007) Structural analysis of conserved oligomeric Golgi complex subunit 2. *J. Biol. Chem.*, **282**, 23418–23426.
37. Whyte, J.R. and Munro, S. (2001) The Sec34/35 Golgi transport complex is related to the exocyst, defining a family of complexes involved in multiple steps of membrane traffic. *Dev. Cell*, **1**, 527–537.
38. Zolov, S.N. and Lupashin, V.V. (2005) Cog3p depletion blocks vesicle-mediated Golgi retrograde trafficking in HeLa cells. *J. Cell Biol.*, **168**, 747–759.
39. Seemann, J., Jokitalo, E., Pypaert, M. and Warren, G. (2000) Matrix proteins can generate the higher order architecture of the Golgi apparatus. *Nature*, **407**, 1022–1026.
40. Mardones, G.A., Snyder, C.M. and Howell, K.E. (2006) Cis-Golgi matrix proteins move directly to endoplasmic reticulum exit sites by association with tubules. *Mol. Biol. Cell*, **17**, 525–538.
41. Bonfanti, L., Mironov, A.A. Jr, Martinez-Menarguez, J.A., Martella, O., Fusella, A., Baldassarre, M., Buccione, R., Geuze, H.J., Mironov, A.A. and Luini, A. (1998) Procollagen traverses the Golgi stack without leaving the lumen of cisternae: evidence for cisternal maturation. *Cell*, **95**, 993–1003.
42. Mironov, A.A., Beznoussenko, G.V., Nicoziani, P., Martella, O., Trucco, A., Kweon, H.S., Di Giandomenico, D., Polishchuk, R.S., Fusella, A., Lupetti, P. *et al.* (2001) Small cargo proteins and large aggregates can traverse the Golgi by a common mechanism without leaving the lumen of cisternae. *J. Cell Biol.*, **155**, 1225–1238.
43. Martinez-Menarguez, J.A., Prekeris, R., Oorschot, V.M., Scheller, R., Slot, J.W., Geuze, H.J. and Klumperman, J. (2001) Peri-Golgi vesicles contain retrograde but not anterograde proteins consistent with the cisternal progression model of intra-Golgi transport. *J. Cell Biol.*, **155**, 1213–1224.
44. Vasile, E., Oka, T., Ericsson, M., Nakamura, N. and Krieger, M. (2006) IntraGolgi distribution of the conserved oligomeric Golgi (COG) complex. *Exp. Cell Res.*, **312**, 3132–3141.
45. Oka, T., Vasile, E., Penman, M., Novina, C.D., Dykxhoorn, D.M., Ungar, D., Hughson, F.M. and Krieger, M. (2005) Genetic analysis of the subunit organization and function of the COG complex: studies of Cog5 and Cog7 deficient mammalian cells. *J. Biol. Chem.*, **280**, 32736–327345.
46. Kim, D.W., Massey, T., Sacher, M., Pypaert, M. and Ferro-Novick, S. (2001) Sgf1p, a new component of the Sec34p/Sec35p complex. *Traffic*, **2**, 820–830.
47. Spasic, D., Tolia, A., Dillen, K., Baert, V., De Strooper, B., Vrijens, S. and Annaert, W. (2006) Presenilin-1 maintains a nine-transmembrane topology throughout the secretory pathway. *J. Biol. Chem.*, **281**, 26569–26577.
48. Mills, P.B., Mills, K., Mian, N., Winchester, B.G. and Clayton, P.T. (2003) Mass spectrometric analysis of glycans in elucidating the pathogenesis of CDG type IIx. *J. Inherit. Metab. Dis.*, **26**, 119–134.
49. Seemann, J., Jokitalo, E.J. and Warren, G. (2000) The role of the tethering proteins p115 and GM130 in transport through the Golgi apparatus *in vivo*. *Mol. Biol. Cell*, **11**, 635–645.